Geology, Geophysics & Environment 2023, vol. 49 (3): 209–224

Diurnal seismic ambient noise and seismic station performance characterization in the Bengal Basin, Bangladesh

Naharin Zannat[1], Atikul Haque Farazi[2], A.S.M. Maksud Kamal[3], Md. Zillur Rahman[4], Md. Shakhawat Hossain[5]

[1] *University of Dhaka, Department of Disaster Science and Climate Resilience, Dhaka, Bangladesh, ORCID ID: 0009-0001-3886-5523*
[2] *University of Barishal, Department of Geology and Mining, Barishal, Bangladesh; Kyoto University, Division of Earth and Planetary Sciences, Kyoto, Japan, ORCID ID: 0000-0002-1822-1421*
[3] *University of Dhaka, Department of Disaster Science and Climate Resilience, Dhaka, Bangladesh, ORCID ID: 0000-0002-3896-2032*
[4] *University of Dhaka, Department of Disaster Science and Climate Resilience, Dhaka, Bangladesh, ORCID ID: 0000-0003-0744-7377*
[5] *University of Dhaka, Department of Disaster Science and Climate Resilience, Dhaka, Bangladesh, e-mail: shakhawat.dsm@du.ac.bd (corresponding author), ORCID ID: 0000-0002-0205-2846*

Received: 23 September 2022; accepted: 12 June 2023; first published online: 15 September 2023

Abstract: Seismic ambient noise (SAN) energy can potentially blur regional and teleseismic arrivals as well as various microearthquakes at specific frequencies. Therefore, quantification of the SAN energy level in a region is required to optimize seismic station distribution for seismological investigations. Moreover, evaluation of station performance and noise source is possible from observation of SAN energy levels. The SAN energy distribution from seismic stations in the Bengal Basin (BB), Bangladesh has not yet been estimated. At the same time, this tectonically active and complex region is less studied using seismic methods. This study aims to quantify SAN energy and characterize its diurnal variation along with evaluating station performance at 11 seismic stations, which were temporarily installed in the deeper portion of the BB. Herein, the daily SAN energy level was determined within the period range of 0.02–30 s by estimating the power spectral density (PSD) of seismic data for 7 continuous days. SAN energy and its variation over time were observed using the probability density functions (PDFs) of PSDs and spectrograms, respectively. The sources of SAN energies at different period bands were also investigated by comparing the PSDs with daily variations in human activities, nearby noise sources, local meteorological factors (i.e., air temperature and precipitation), and sea level height. The insights from this study could be useful for the future deployment of seismic networks as well as seismological studies in the BB.

Keywords: seismic ambient noise, power spectral density, noise energy, noise sources, seismic station, Bengal Basin

INTRODUCTION

Omnipresent small amplitude seismic waves recorded by seismometers due to tiny ground vibrations, induced by natural (e.g., ocean waves, winds, etc.) or anthropogenic (e.g., traffic, industry, etc.) activities, are termed seismic ambient noise (SAN) (Peterson 1993, Webb 1998, Rahman et al. 2018, Nakata et al. 2019, Lecocq et al. 2020, Farazi et al. 2023b). Long-period (generally >1 s)

SAN are termed microseisms (Webb 1998, Ardhuin et al. 2015), whereas short-period (generally <1 s) SAN are termed microtremors (Molnar et al. 2018). Based on recordings of onshore seismic stations worldwide, Peterson (1993) presented a global noise model with a new high noise model (NHNM) and a new low noise model (NLNM) in terms of power spectral density (PSD), which has been accepted globally and described by many authors from both onshore (e.g., McNamara & Buland 2004, Vassallo et al. 2012) and offshore study environments (e.g., Webb 1998, Nishida 2017, Farazi et al. 2023b). Two distinct peaks are observed on the NHNM above 1 s period bands, known as double frequency peak (within 1–10 s) and single-frequency peak (within 10–20 s), governed by secondary and primary microseism frequency bands, respectively (McNamara & Buland 2004, Nishida 2017). The double-frequency peak is generated when two oppositely traveling ocean waves of similar frequency are superimposed together to produce standing gravity waves (Longuet-Higgins 1950). The single-frequency peak is related to the seismic energy converted from vertical pressure variation or the interaction of waves with the shallow sea floor (Hasselmann 1963). These two peaks are identified at almost all of the seismic stations, with their amplitude may vary and even shifting slightly from place to place (Pierson & Moskowitz 1964, Marzorati & Bindi 2006). These peaks are also observed at onshore stations, hundreds or thousands of kilometers from the shore because energy from these frequency bands is brought by Rayleigh propagation, but with increasingly lower amplitude with distance from the shore (Webb 1998, McNamara & Buland 2004, Baker et al. 2019).

When the main purpose of a seismic network is to record and provide data for monitoring seismic activities, studying seismic sources and the structure of the earth, contamination of the seismograph recordings by SAN energy makes it difficult to analyze data for earthquake monitoring by reducing the signal to noise ratio (SNR) (Grecu et al. 2018). Therefore, reducing noise levels from seismograms greatly increases the quality of seismic data (McNamara & Buland 2004). Hence, to provide high-quality data to researchers and international seismological data centers for seismological studies, seismic network operators usually try to reduce seismic noise (Grecu et al. 2018). Therefore, the first step in reducing noise levels is the precise quantification of noise by analyzing it. Quantification and characterization of SAN can provide important insights into the detectability of seismic events at a station as well as station performance (Marzorati & Bindi 2006, Demuth et al. 2016).

Peterson (1993) established the most common procedure of computing SAN levels by only choosing the quiet periods from the seismic traces. This method was extended by McNamara & Buland (2004) by using the whole seismic record including the transient signals, which facilitated the observation of the distribution of the SAN levels for the entire frequency range over long periods of time. Therefore, both SAN levels and seismic station performance can be observed utilizing this method.

In this study, we quantified diurnal SAN energy levels from PSDs and their geographic variations in the Bengal Basin (BB), Bangladesh (Fig. 1) from seismic recordings of 7 consecutive days at 11 seismic stations. Performance of these seismic stations was also evaluated from the PSDs. We also assessed the impact of daily human activities, meteorological factors (i.e., air temperature and precipitation) and sea level on the PSDs of different period bands. The results of this study could provide useful insights for the deployment of future seismic stations in Bangladesh.

TECTONIC SETTING

Bangladesh occupies most of the part of the BB (Alam 1989) that tectonically lies near the junction of the Indian, Eurasian, and Burmese plates (Alam et al. 2003) (Fig. 1). The Eurasian-Indian plate boundary forms the Himalayan Arc, whereas the Indian-Burmese plate boundary forms the Burma Arc (Ni et al. 1989). The Himalayan and Burmese arcs override the Indian Plate from the north and from the east, respectively, to form their respective foreland basins: the Assam Basin and the BB (Steckler et al. 2008, 2016). The Shillong Plateau, a sliver of the Indian Craton ahead of the Himalayan front, overthrusts toward the south on the BB causing the rapid subsidence of the Surma basin, a sub-basin in the NE BB as well

as NE Bangladesh (Johnson & Alam, 1991, Khan & Chouhan 1996). Active obduction of the Burma Arc with the large sediment loads of the Ganges-Brahmaputra-Meghna (GBM) delta forms a huge accretionary prism and fold-belt – Indian-Burman Ranges (IBR), the western extension of which in Bangladesh is the Chittagong-Tripura fold-belt (CTFB, Alam et al. 2003). The fold-belt is exposed in the SE Bangladesh with an average elevation of around 1100 m (Bürgi et al. 2021), but is still blindly extending westward into the low lying GBM delta (Steckler et al. 2008).

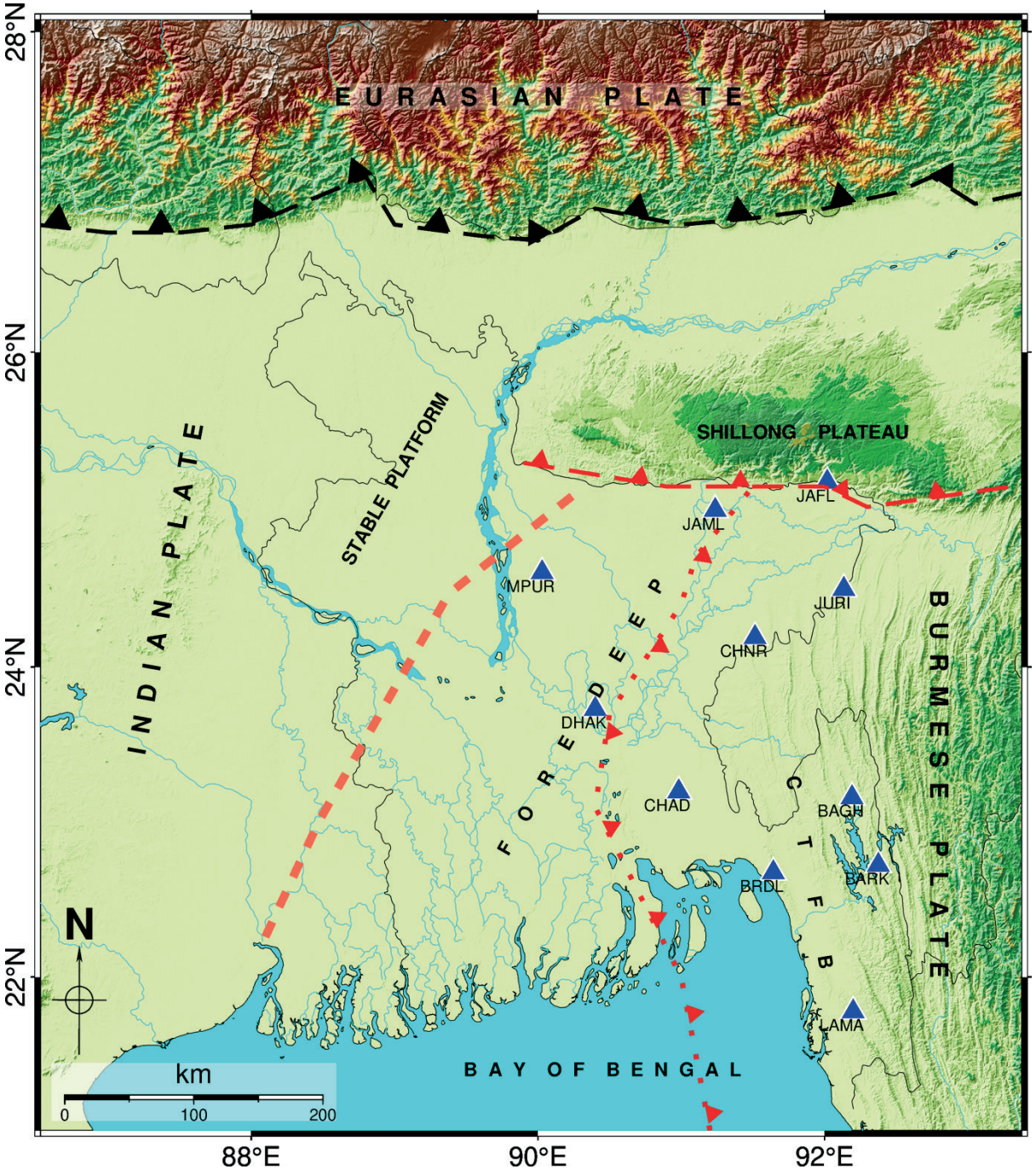

Fig. 1. *Map of BB, Bangladesh is showing its tectonic framework with the seismic stations used in this study (indicated by blue triangles with station code below). The tectonic elements were taken from (Alam et al. 2003, Steckler et al. 2016). Red dashed line: the Dauki Fault; red dotted line: the inferred Indian-Burmese plate boundary megathrust fault; thick red dashed line: the Eocene Hinge Zone. The barbs with the lines indicate the subduction direction. CTFB: Chittagong-Tripura fold-belt*

Recently, Mahmud et al. (2020) have suggested that the lower Meghna River in southern Bangladesh could indicate the Indian-Burmese plate boundary fault.

The BB could be subdivided into three distinct tectonic provinces: (i) the stable platform on the east, (ii) the foredeep in the center of BB, and (iii) the CTFB (Fig. 1; Alam et al. 2003). The first two tectonic provinces are demarcated by the Eocene Hinge Zone. While sediment thickness is thin in the stable platform (~0.2–6 km), it varies from ~3–20 km in the rest of the tectonic provinces (Alam et al. 2003, Singh et al. 2016). In this study, we consider the foredeep and the CTFB tectonic provinces together as the "deep basin" portion of the BB. The active tectonics and the past earthquake records (Bilham 2004) in and around Bangladesh supports the specter of an impending mega-quake (Singh et al. 2016, Farazi et al. 2018, Hossain et al. 2020, Bürgi et al. 2021, Farazi et al. 2023a), therefore, demanding rigorous geophysical and seismological studies for precisely evaluating the tectonic and geodynamic setting of this region.

INSTRUMENTATION AND DATA

To delineate the sedimentary and crustal structure in the GBM delta, a network of seismic sensors named "Z6" was deployed for the period between 2011 and 2015 and operated by Lamont Doherty Earth Observatory (LDEO), Columbia University (FDSN 2011)). Another single station, station code: DHAK, has been in operation since 2008 with the network name "BI" (FDSN 2008). These stations rest on the deep basin part (i.e., foredeep and CTFB) of the BB. Herein, we used vertical component data of 11 stations from these networks (Fig. 1). The sampling frequency of these sensors was 100 Hz.

For this study, digital seismic time series data were downloaded using ObsPy, a Python package for seismology (Beyreuther et al. 2010), from the website of Incorporated Research Institutions for Seismology (IRIS). This study utilized a continuous time series trace of 7 consecutive days. The data acquisition period from station to station varied based on availability of continuous data for 7 days. Information about the sensors and the data period is provided in Table 1.

Table 1
Station code, length of data, instrument/datalogger information, sensor type, and flat response of each sensor of every station used in this study

Station code	Data period	Instrument/datalogger	Sensor type	Flat response [Hz]
DHAK	1.01.2014 – 30.04.2014	Kinemetrics SV1-SH1/ Reftek 72A-02 Datalogger	intermediate	0.03–50
BAGH	1.01.2015 – 30.04.2015	Mark Products L4C/ Reftek 130 Datalogger	short-period	1.0–50
BARK	1.01.2015 – 30.04.2015	Mark Products L4C/ Reftek 130 Datalogger	short-period	1.0–50
BRDL	1.01.2015 – 30.04.2015	Guralp CMG40T/ Reftek 130 Datalogger	intermediate	0.03–50
CHAD	1.01.2015 – 30.04.2015	Mark Products L4C/ Reftek 130 Datalogger	short-period	1.0–50
CHNR	1.01.2014 – 30.04.2014	Guralp CMG40T/ Reftek 130 Datalogger	intermediate	0.03–50
JAFL	1.01.2015 – 30.04.2015	Guralp CMG40T/ Reftek 130 Datalogger	intermediate	0.03–50
JAML	1.01.2015 – 30.04.2015	Guralp CMG40T/ Reftek 130 Datalogger	intermediate	0.03–50
JURI	1.01.2015 – 30.04.2015	Guralp CMG40T/ Reftek 130 Datalogger	intermediate	0.03–50
LAMA	1.01.2014 – 30.04.2014	Guralp CMG40T/ Reftek 130 Datalogger	intermediate	0.03–50
MPUR	1.01.2015 – 30.04.2015	Guralp CMG40T/ Reftek 130 Datalogger	intermediate	0.03–50

Daily temperature and precipitation data were collected at 3 hour intervals from the Bangladesh Meteorological Department (BMD). Daily variation of relative sea level height, measured by a tide gauge station (CHITTAGONG A) in Chittagong, was collected from Permanent Service for Mean Sea Level (PSMSL, https://psmsl.org/).

METHOD

For SAN energy estimation, we used the probabilistic power spectral density (PPSD) and spectrogram proposed by McNamara and Buland (2004), that employs power spectral density (PSD) and probability density function (PDF) to show variations in SAN levels. The analysis was performed within 0.02–30 s period range. It is proven that SAN travels mostly as Rayleigh waves from its source to a distant seismic station (Webb 1998, Campillo and Paul 2003, Shapiro et al. 2005), therefore, herein we use only the vertical component data.

In the PPSD routine of McNamara & Buland (2004), PSDs are computed using the algorithm utilized by Peterson (1993) and they are then used to define the PDF of noise for a station. The advantage of this method is that there is no need to screen the data for earthquakes, gaps, spikes, calibrations pulses, etc. as these signals in the seismic data have a low-probability of occurrence and do not usually contaminate high-probability noise (McNamara & Buland 2004).

The PSD (P_k) was computed by squaring the Fourier amplitude spectrum (Y_k) of the time series data and normalizing by twice the ratio of the sampling interval Δt to the number of samples (N) (McNamara & Buland 2004):

$$P_k = \frac{2\Delta t}{N}\left|Y_k\right|^2 \tag{1}$$

Finally, the PSD was obtained in decibels [dB] with respect to acceleration of 1 $(m/s^2)^2$/Hz. To statistically analyze the SAN energy variation over a particular period, PDFs were computed for each PSD curve by smoothing with a centered-average moving window having a width of 1/8 of an octave. The PSD values at each period were then assembled into 1-decibel bins for estimating recurrence of PSD of each period using a histogram. At last, the PDF was built by normalizing the histogram period by period. Figure 2 shows the PPSD plots of 7 continuous days obtained from this study. In addition, to discern diurnal SAN energy variation, a spectrogram of PSDs was also generated for a single day (Fig. 3) and for 7 days (Fig. 4).

We also analyzed the daily PSDs of SAN energy at three seismic stations, JAFL, DHAK and BRDL in Sylhet, Dhaka and Chittagong, respectively, and we compared daily PSD energy variation with human activities, local meteorological factors (i.e., temperature and precipitation) and sea level height, obtained from a tide gauge station (Figs. 5–8, respectively), to find possible energy sources and their effects on seismometer recordings in the study area. The selected stations were in three different tectonic zones of Bangladesh (Farazi et al. 2023a). The PSD amplitude values of the selected period bin were normalized with a three-hour moving window. Generally, the SAN wavefield below the 1 s period is excited by anthropogenic activities, around the 1 s period is excited by wind effects and local meteorological factors, and above the 1 s period is excited by oceanic and broad-scale meteorological factors (Webb 1998, McNamara & Buland 2004, Bonnefoy-Claudet et al. 2006, Marzorati & Bindi 2006, Lecocq et al. 2020, Farazi et al. 2023b). Therefore, energy variations of period bands 0.34–0.71 s (central period 0.5 s) and 0.7–1.4 s (central period 1 s) were compared with day and night times of an entire week (Fig. 5). Moreover, the SAN energy of period band 0.7–1.4 s (central period 1 s) was compared with daily temperature and precipitation records throughout an entire week (Figs. 6, 7). Additionally, energies of period band 0.7–1.4 s (central period 1 s) and 4.3–8.6 s (central period 6 s) were compared with diurnal sea level variation (Fig. 8).

RESULTS AND DISCUSSION

This study presents SAN energy levels at 11 stations in the deep basin portion of BB, Bangladesh in terms of PPSD distribution (Fig. 2) along with daily (Fig. 3) and weekly variation (Fig. 4). In this section, we will detail the SAN power level and diurnal variation for the period bands 20–30 s, 10–20 s, 1–10 s, 0.02–1 s separately.

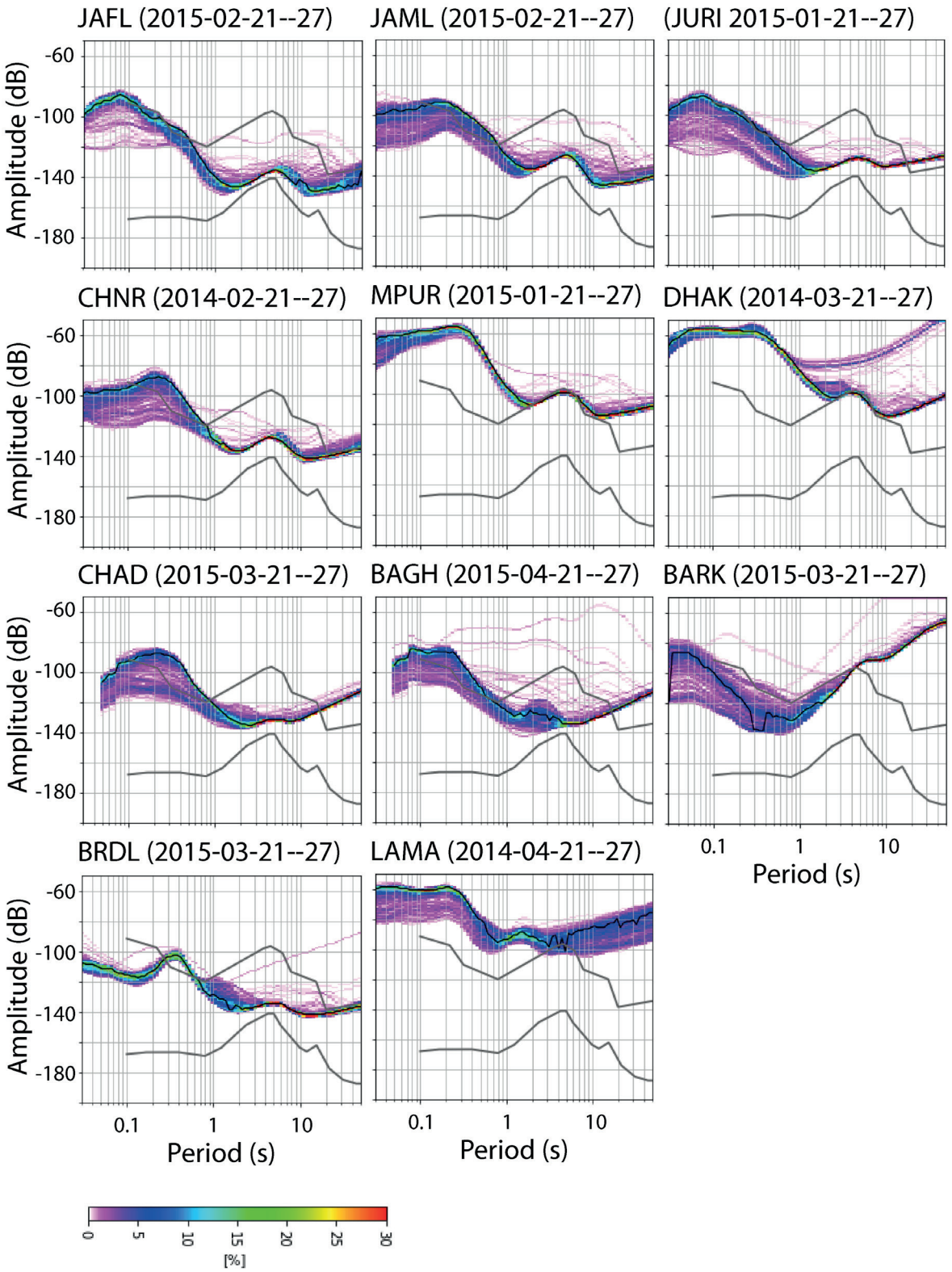

Fig. 2. *PPSD plots demonstrating PSD-PDFs of 7 consecutive days of seismic recordings of the vertical component from all the stations used in this study (Fig. 1). From top to bottom, the stations' distance decreases from the shoreline in southern Bangladesh. The energy mode of the observed PSDs is presented by solid black line. X-axis shows periods in seconds [s] and Y-axis shows SAN energy in decibels [dB]. The color bar at the right of each PPSD plot represents probability of occurrence of a given energy at a certain period. Station code and date range are provided on top of each panel. The NHNM (upper gray solid line) and the NLNM (lower gray solid line) of Peterson (1993) are also shown*

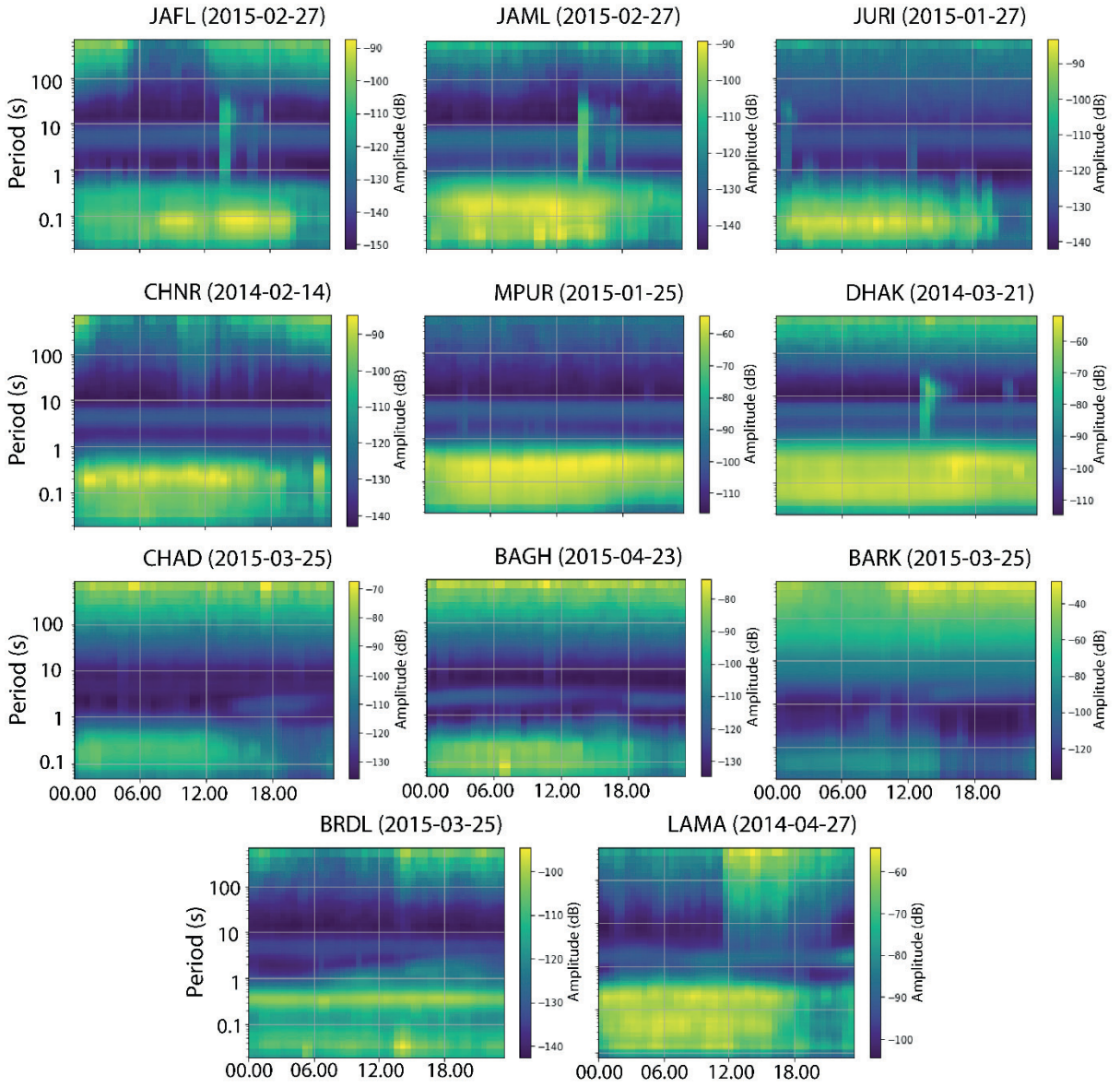

Fig. 3. *24-hours PSD spectrograms (daily spectrograms) of the vertical components of the seismic stations presented in Figure 2. The Y-axis presents the hours of a day. Station code and date are above each spectrogram*

Long period band (20–30 s)

The maximum flat response of the intermediate sensors is 33 s; therefore, we consider the 20–30 s period band SAN herein. Apart from stations JAFL, JAML, CHNR, and BRDL, the PDF mode of the PSDs as well as almost all the PSDs for 7 days at all other stations exceed the NHNM in this period band (Fig. 2). However, the BAGH, BARK, and CHAD stations are short-period stations, therefore the noise energy exceeding the NHNM is the background noise from sensor self-noise.

In this period band, the daily spectrograms show that the SAN energy varies from around –140 dB to around –105 dB at CHNR, JAFL, and JURI and from around –110 dB to around –40 dB at the rest of the stations (Fig. 3). The higher energy is especially evident from around 12.00 p.m. to around 12.00 a.m.

In the weekly spectrograms, the stations JAFL, JAML, CHNR, and BRDL exhibit SAN energy variation from around –150 dB to around –120 dB, while the rest of the stations exhibit variation from around –150 dB to –60 dB (Fig. 4).

Herein, some higher energy patches are related to seismic events, which are observed in the PPSD plots. However, no mentionable diurnal cycle of SAN power variation throughout the week is observed within this period band.

In this period band, SAN is usually generated by an oceanic infragravity wave (Webb 1998), which contains high energy, but the energy is reduced at the inland stations with increasing distance from the shore. However, in this period band, high energy at an onshore station could be induced by tilting owing to either weather conditions or poor station design and could be indicated by smearing on the PPSD plot (McNamara & Buland 2004, Uthaman et al. 2022).

Primary band (10–20 s)

In this period band, the PSD curves exceed the NHNM at MPUR, DHAK and LAMA (Fig. 2). Stations BAGH, CHAD and BARK are equipped with short-period sensors that do not allow the reliable measurement of SAN energy within this period range.

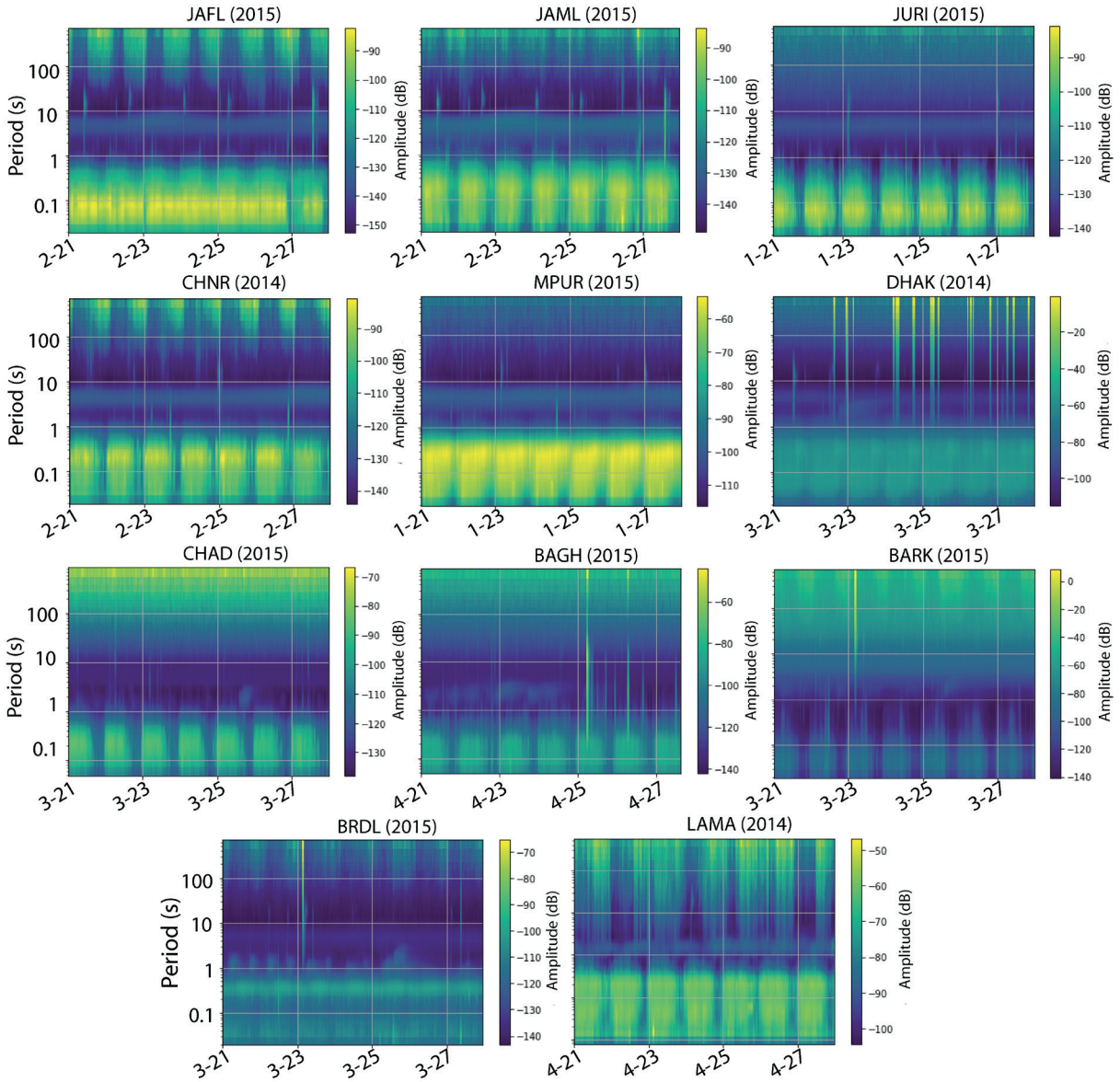

Fig. 4. *7-day PSD spectrograms (weekly spectrograms) of the vertical components of the stations are presented in Figures 2 and 3. The Y-axis presents the time in month-day. The station code and year are above each spectrogram*

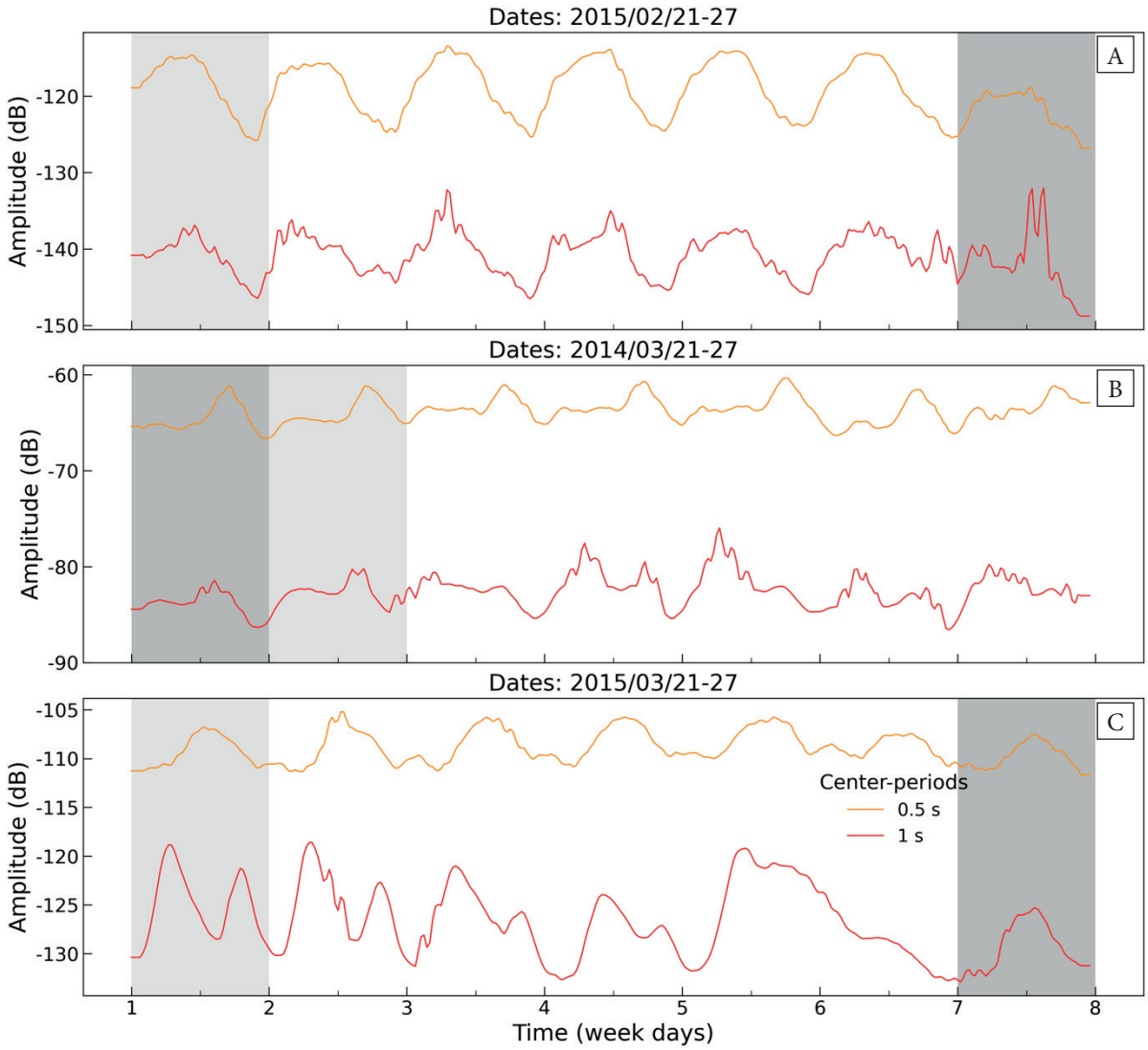

Fig. 5. *PSD amplitudes of period bands 0.34–0.71 s (central period 0.5 s) and 0.7–1.4 s (central period 1 s) as a function of time for 7 continuous days. Stations JAFL, DHAK and BRDL are in A, B and C, respectively. The dark-gray and light-gray shaded portions mark the weekends in Bangladesh, i.e., Friday and Saturday, respectively. The entire time period is similar to those in Figures 2 and 4*

The other stations – JAFL, JURI, CHNR, JAML and BRDL – exhibit PSDs within the global noise models of Peterson (1993, Fig. 2). Among these stations, only the JAFL station shows the typical low amplitude single frequency peak within this period band.

Energy level in this period band depends on the weather condition, and the single frequency peak is generated due to energy from distant storms in the ocean (Nishida 2017). Therefore, the presence or absence of such a peak at stations with the intermediate flat response could be related to either the observation time or the performance of the sensor.

The intermediate sensors have energy variations from around –140 dB to around –130 dB without any significant variation throughout the day and PSDs are within the global noise models (Fig. 3). On the weekly spectrograms (Fig. 4), the energy level ranges from around –150 dB to around –140 dB without any prominent diurnal cycle. The sharp energetic spikes in this period band are probably caused by surface waves from earthquakes (McNamara & Buland 2004).

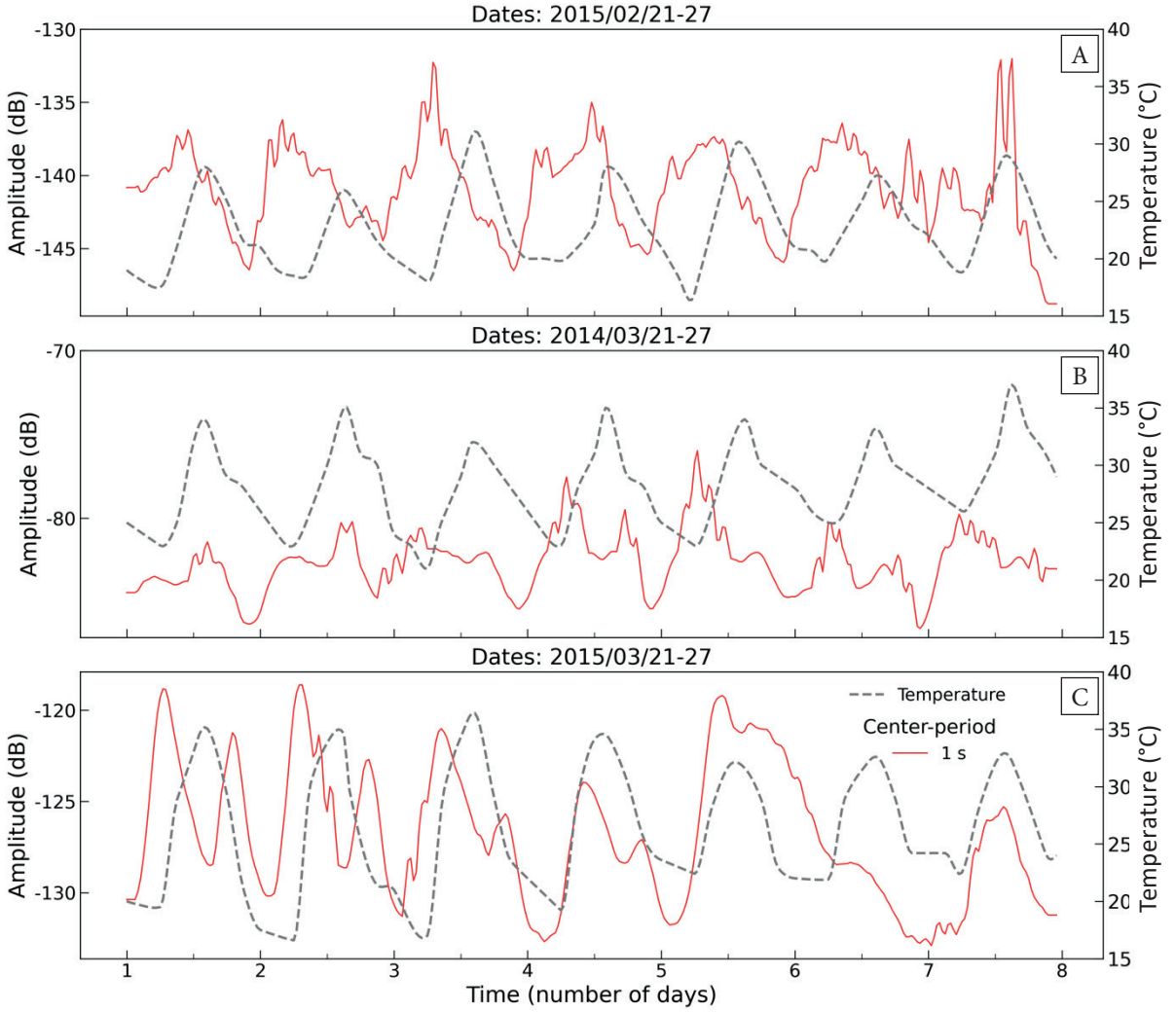

Fig. 6. *PSD amplitudes of period bands 4.3–8.6 s (center period 6 s) and 10–20s (center period 15 s) are presented with temperature record and as a function of time for 7 continuous days. Stations JAFL, DHAK and BRDL are in A, B and C, respectively. The entire time period is similar to those in Figures 2 and 4*

Secondary band (1–10 s)

In this period band, a double frequency peak is observed at all the stations (Fig. 2). Among all the stations, only LAMA exhibits PSDs overshooting the NHNM. LAMA is situated near the Matamuhuri River by ~0.6 km and near the shore by ~30 km. The higher energy in this period band could be caused by the river flow if it is not the sensor's self-noise (Burtin et al. 2008, Uthaman et al. 2022). Daily spectrograms show SAN level variation from around –150 dB to –120 dB without any variation throughout the observed day, except at BRDL (Fig. 3). At BRDL, SAN energy increases from around –140 dB at 12.00 a.m. to around –120 dB within 8 to 10 after almost 15.00 p.m. This station is very close to the shore (~7 km), therefore, oceanic energy within the wavelength of this period may contribute to such energy variation (Fig. 8). This diurnal cycle is also visible on the weekly spectrogram of BRDL (Fig. 4). There is more discussion on the SAN source of this period band at BRDL in Section "Analyzing noise sources." However, in this period band, no mentionable diurnal energy variation cycle was discerned on the weekly spectrograms of the rest of the stations (Fig. 4). The occasional energetic spikes in this period band are probably caused by surface and/or body waves from earthquakes (McNamara & Buland 2004).

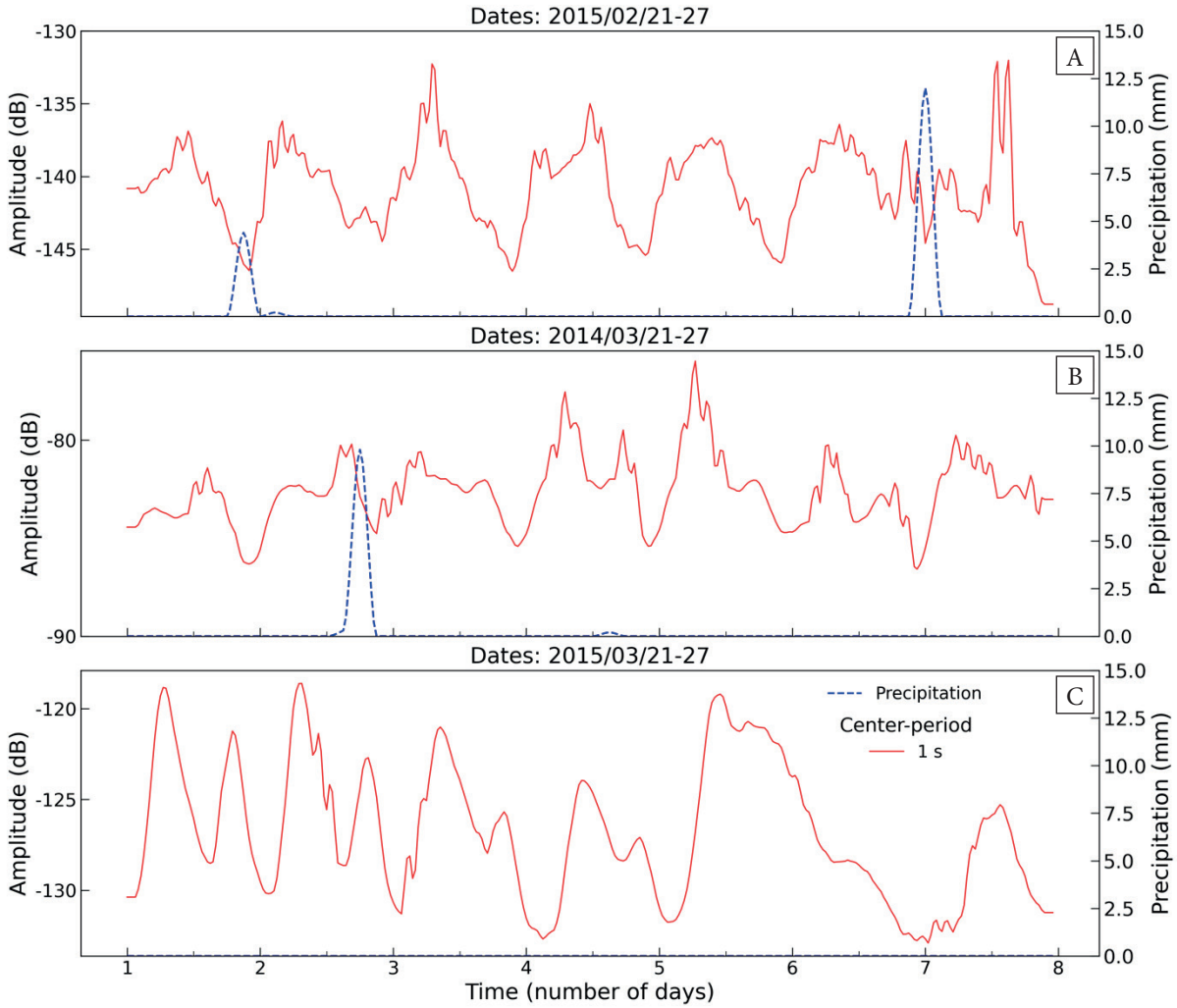

Fig. 7. *PSD amplitudes of period bands 4.3–8.6 s (center period 6 s) and 10–20 s (center period 15 s) are presented with precipitation record and as a function of time for 7 continuous days. Stations JAFL, DHAK and BRDL are in A, B, C, respectively. The entire time period is similar to those in Figures 2 and 4*

Short-period band (0.02–1 s)

Within this period band, an increasing trend of the PSD energy mode is observed at all the stations forming a peak within 0.03 to 0.3 s. At all the stations, the power mode of the PSDs varies from around –100 dB to around –60 dB. Among them, DHAK, MPUR, and LAMA exhibit the peak energy level almost over 60 dB and substantially overshoots the NHNM. The SAN energy modes of the rest of the stations are either below the NHNM or marginally overshoot it. DHAK is situated at the University of Dhaka, a very busy area in the capital city Dhaka, Bangladesh, which is severely affected by traffic noise and many other human activities. Therefore, energetic cultural noise is expected at this station. MPUR is located near the Dhaka-Mymensingh highway (~0.3 km), thus heavy traffic could be the source of the high energy measured here. At LAMA, high short-period energy could be caused by the flow in the nearby Matamuhuri River (~0.6 km, Burtin et al. 2008, Uthaman et al. 2022).

The daily spectrograms of all of the stations display a sharp energy increase usually around 0.5 s that continues up to 0.02 s. JAFL demonstrates energy increase from around –100 dB to around –85 dB from almost 9.00 a.m. to almost 21.00 p.m. MPUR and DHAK manifest nearly –50 dB energy level throughout the day.

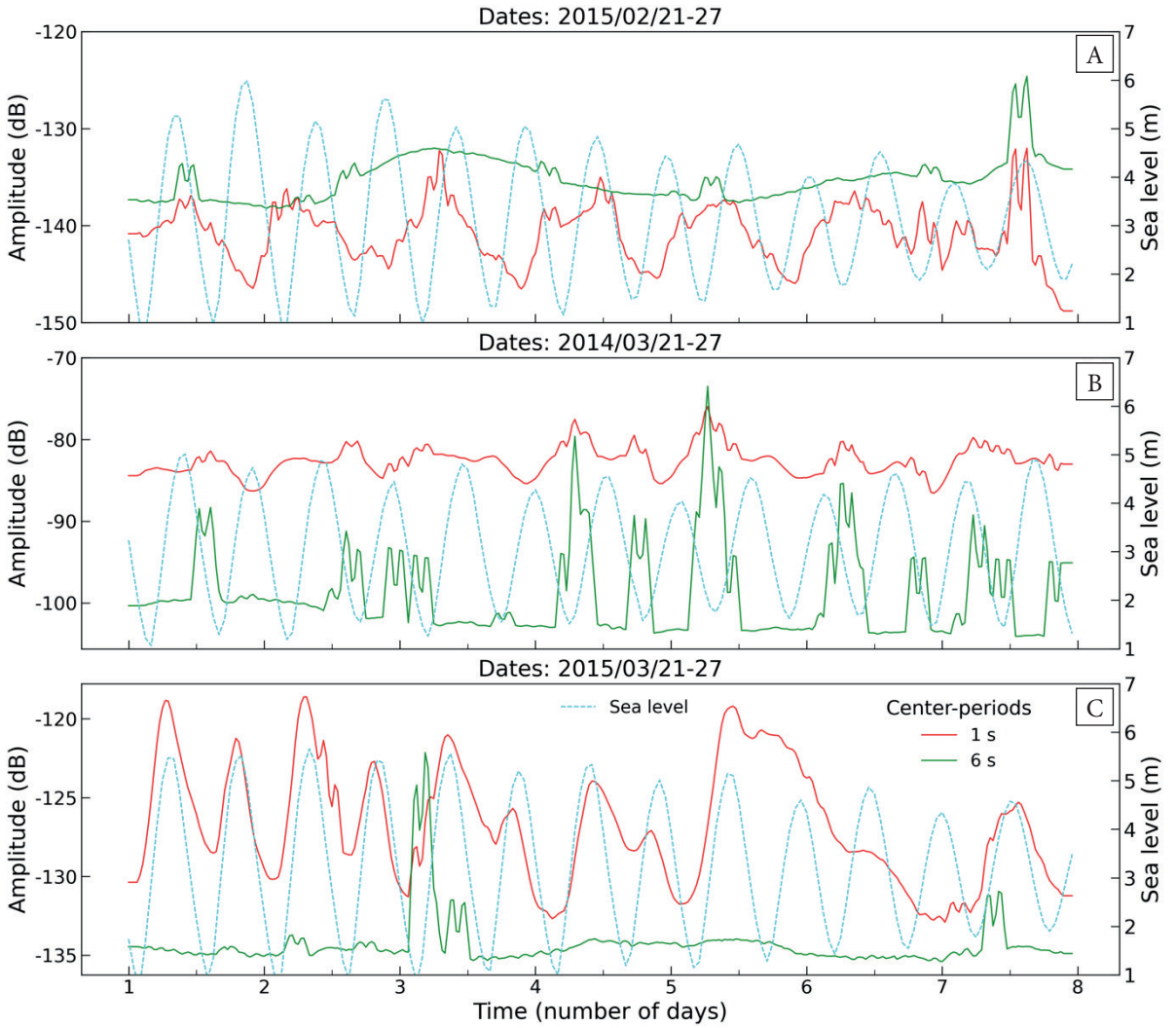

Fig. 8. *PSD amplitudes of period bands 0.7–1.4 s (central period 1 s) and 4.3–8.6 s (center period 6 s) are presented with hourly sea level record and as a function of time for 7 continuous days. Stations JAFL, DHAK and BRDL are in A, B, C, respectively. The entire time period is similar to those in Figures 2 and 4*

At the rest of the stations, the SAN energy is nearly –100 dB to –80 dB from almost 12.00 a.m. to almost 18.00 p.m., which then decrease to around –130 dB to around –120 dB within the remaining time of the day.

The diurnal cycle of SAN energy variation is observed on the weekly spectrograms of all the stations, especially within the cultural noise band (0.1–1 s, Fig. 4). Very high energy is seen usually below 0.5 s period. The possible causes of such high energy could be related to poor performance of the sensors or even noise from the power supply generator at some remote stations (e.g., JAFL). Moreover, all the stations are located either near highways [BRDL (~1.6 km), DHAK (~0.12 km), and MPUR (~0.3 km)], local roads [CHNR (~0.1 km) and JURI (~0.08 km)] or near rivers [BAGH: Kachalang River (0.2 km); BARK: Karnaphuli River (~0.1 km); CHAD: the Padma River (~0.8 km); CHNR: Khowai and Sutang rivers to the east and west, respectively (~1.7 km both); JAFL: Goyain River (~0.5 km); JAML: Surma River (~0.05 km); JURI: Juri River (~1.6 km); LAMA: Matamuhuri River (~0.06 km)], which make the stations susceptible to less attenuated, energetic cultural noise. Further discussion on short-period energy variation and noise source are provided in Section "Analyzing noise sources."

All the stations of this study were installed in surface vaults, thus providing susceptibility to sort-period cultural noise. The short-period SAN energies exceeding the NHNM could potentially hinder future micro- and slow-earthquake detections in the study area. Measurements of decreasing cultural noise energy on a seismic station could be taken by placing a sensor on a hard site or installing in a borehole, but in a deep sedimentary basin like the BB, hard sites are rarely found. Therefore, to get rid of the short-period high energy noise in the study area, seismic stations are required to be installed in places avoiding highways and rivers, and in boreholes if possible.

Analyzing noise sources

In this study, different noise sources were verified at three representative seismic stations located at three distant parts of the BB (Farazi et al. 2023a). Short-period SAN wavefields (generally ≤1 s) primarily consist of anthropogenic noise propagating mainly as high-frequency surface waves and attenuating within distances and depths of several kilometers (McNamara & Buland 2004, Bonnefoy-Claudet et al. 2006, Marzorati & Bindi 2006, Lecocq et al. 2020). Therefore, daily anthropogenic activities leave an imprint on the seismometer records of these period bands. All three stations in Figure 5 show variations in the diurnal SAN energy pattern for period bands 0.34–0.71 s (central period 0.5 s) and 0.7–1.4 s (central period 1 s). It is quite evident that daily SAN energy is maximum at midday and minimum at midnight in a cyclic pattern throughout a week, indicating a cultural noise source. Very high noise levels in station DHAK compared to the others indicate that it is nearby a very busy and crowded place (i.e., University of Dhaka) in the capital city Dhaka. SAN levels in the weekends also exhibit similar pattern probably because all three stations are nearby popular places for visitors during the holidays. The almost constantly high energy flattening the peak of the 0.5 s central period band at JAFL could be caused by the runoff in the nearby Goyain River (200 m from JAFL) (Burtin et al. 2008, Uthaman et al. 2022). The 1 s central period band at BRDL shows different behavior than the rest of the stations, which we will discuss here later.

SAN around 1 s is generated due to coupling of the ground with wind induced velocity and other local meteorological conditions (Bonnefoy-Claudet et al. 2006). External meteorological conditions (i.e., air temperature and precipitation) could affect SAN wavefield of around 1 s period band (Colombero et al. 2018, Oakley et al. 2021). Figures 6 and 7 show comparison of 0.7–1.4 s (central period 1 s) period band daily SAN energy variation with temperature and precipitation, respectively. Overall, temperature increase correlates well with SAN energy increase for some day at all three stations, while it is not the case in some other days. Therefore, no definite conclusions could be drawn from this observation. Precipitation has no correlation at all with SAN energy increase or decrease.

Microseism bands (1–10 s) are generated in the oceans and controlled by atmospheric and weather conditions (Hasselmann 1963, Webb 1998, McNamara & Buland 2004, Bonnefoy-Claudet et al. 2006, Farazi et al. 2023b). Figure 8 represents a correlation of relative sea level variation due to tidal effect with SAN energy variations in period bands 0.7–1.4 s (central period 1 s) and 4.3–8.6 s (center period 6 s). No evidence of a correlation was obtained apart from a 1 s period band at BRDL. JAFL and DHAK are far away from the shoreline and thus low microseism energy is expected at these stations. BRDL is only 7 km away from the coast, SAN energy around 1 s period exhibit formation of 2 peaks every day which strongly correlates with diurnal sea level variation. Therefore, it is evident that sea level variation can be monitored from near shore seismic stations.

The insights obtained from diurnal SAN energy variation along with contribution from different noise sources could be useful for future seismic station installation and seismic monitoring in the deep basin area of the sedimentary BB, Bangladesh. Further analysis on long term seasonal SAN energy variation could bear a more comprehending understanding of the nature of the noise wavefield in the thickest and largest sedimentary basin in the world.

CONCLUSIONS

Based on PSD analysis, characteristics of seismic ambient noise (SAN) at 11 seismic stations were estimated in the deeper part of the BB, Bangladesh in terms of diurnal variation of SAN energy within the 0.02–30 s period range. The study revealed that PSDs and energy modes of PSDs of some stations (i.e., BRDL, CHNR, DAK, MPUR, JAFL, JAML, JURI, and LAMA) within 10–30 s were overshooting the NHNM likely because of poor station performance. At some stations (i.e., BARK, DHAK and LAMA), the PSDs and energy modes of the 1–10 s period band were marginally overshooting the NHNM probably due to station performance. Within the 0.02–1 s period band (short-period band) high energies above the NHNM are observed generally below 0.5 s at all the stations, which could be related to sensors' self-noise, river flow, heavy traffic or power supply generators. At the rest of the stations, SAN energy, within the 0.02–30 s period range, was within the NHNM and NLNM indicating satisfactory station performance. Daily and weekly spectrogram analysis manifested diurnal variation in noise energy prominently within the short-period band (0.1–1 s). Moreover, examination of SAN energies of 0.5 s and 1 s period bin at BRDL, DHAK and JAFL exhibited a repeating diurnal cycle. Among them, SAN energy of 1 s period at BRDL exhibited diurnal variation with sea level. No mentionable effect of temperature and precipitation was discerned on noise energy of 1 s period.

To avoid energetic short-period cultural noise for future earthquake detection studies, we recommend installing seismic sensors in boreholes as week as avoiding nearby highways and rivers. Despite a complicated and active tectonic setting with highly destructive seismogenic potential, the BB is still a seismically understudied region of the world. This study provides important insights into seismic station performance and some noise sources in the deep sedimentary portion of BB from observation of diurnal SAN energy variation. Therefore, this study would be informative for future seismic station deployment in this region. Future work could be devoted to revealing any seasonal variation of SAN energy for the more comprehensive characterization of SAN in the BB.

We are thankful to the Department of Disaster Science and Climate Resilience, University of Dhaka, Bangladesh for supporting this study. We are grateful to Bangladesh Meteorological Department (BMD) for providing air temperature and rainfall data. We also used sea level data from Permanent Service for Mean Sea Level (PSMSL). We would also like to express our gratitude to the two anonymous reviewers for their valuable suggestions which helped improve the manuscript.

REFERENCES

Alam M., 1989. Geology and depositional history of Cenozoic sediments of the Bengal Basin of Bangladesh. *Palaeogeography, Palaeoclimatology, Palaeoecology*, 69(C), 125–139. https://doi.org/10.1016/0031-0182(89)90159-4.

Alam M., Alam M.M., Curray J.R., Chowdhury M.L.R. & Gani M.R., 2003. An overview of the sedimentary geology of the Bengal Basin in relation to the regional tectonic framework and basin-fill history. *Sedimentary Geology*, 155(3–4), 179–208. https://doi.org/10.1016/S0037-0738(02)00180-X.

Ardhuin F., Gualtieri L. & Stutzmann E., 2015. How ocean waves rock the Earth: Two mechanisms explain microseisms with periods 3 to 300 s. *Geophysical Research Letters*, 42(3), 765–772. https://doi.org/10.1002/2014GL062782.

Baker M.G., Aster R.C., Anthony R.E., Chaput J., Wiens D.A., Nyblade A., Bromirski P.D. et al. 2019. Seasonal and spatial variations in the ocean-coupled ambient wavefield of the Ross Ice Shelf. *Journal of* Glaciology, 65(254), 912–925. https://doi.org/10.1017/jog.2019.64.

Beyreuther M., Barsch R., Krischer L., Megies T., Behr Y., Wassermann J., 2010. ObsPy: A Python Toolbox for Seismology. *Seismological Research Letters*, 81(3), 530–533. https://doi.org/10.1785/GSSRL.81.3.530.

Bilham R., 2004. Earthquakes in India and the Himalaya: Tectonics, geodesy and history. *Annales Geophysicae*, 47(2–3), 839–858. https://doi.org/10.4401/ag-3338.

Bonnefoy-Claudet S., Cotton F. & Bard P.-Y., 2006. The nature of noise wavefield and its applications for site effects studies. *Earth-Science Reviews*, 79(3–4), 205–227. https://doi.org/10.1016/j.earscirev.2006.07.004.

Bürgi P., Hubbard J., Akhter S.H. & Peterson D.E., 2021. Geometry of the Décollement Below Eastern Bangladesh and Implications for Seismic Hazard. *Journal of Geophysical Research: Solid Earth*, 126(8), e2020JB021519. https://doi.org/10.1029/2020JB021519.

Burtin A., Bollinger L., Vergne J., Cattin R. & Nábělek J.L., 2008. Spectral analysis of seismic noise induced by rivers: A new tool to monitor spatiotemporal changes in stream hydrodynamics. *Journal of Geophysical Research: Solid Earth*, 113(B5), 5301. https://doi.org/10.1029/2007JB005034.

Campillo M. & Paul A., 2003. Long range correlations in the diffuse seismic coda. *Science*, 299(5606), 547–549. https://doi.org/10.1126/SCIENCE.1078551.

Colombero C., Baillet L., Comina C., Jongmans D., Larose E., Valentin J. & Vinciguerra S., 2018. Integration of ambient seismic noise monitoring, displacement and meteorological measurements to infer the temperature-controlled long-term evolution of a complex prone-to-fall cliff. *Geophysical Journal International*, 213(3), 1876–1897. https://doi.org/10.1093/GJI/GGY090.

Demuth A., Ottemöller L. & Keers H., 2016. Ambient noise levels and detection threshold in Norway. *Journal of Seismology*, 20(3), 889–904. https://doi.org/10.1007/S10950-016-9566-8/FIGURES/10.

Farazi A.H., Ferdous N. & Kamal A.S.M.M., 2018. LPI based earthquake induced soil liquefaction susceptibility assessment at Probashi Palli Abasan Project Area, Tongi, Gazipur, Bangladesh. *Journal of Scientific Research*, 10(2), 105–116. https://doi.org/10.3329/jsr.v10i2.34225.

Farazi A.H., Hossain M.S., Ito Y., Piña-Flores J., Kamal A.S.M.M. & Rahman M.Z., 2023a. Shear wave velocity estimation in the Bengal Basin, Bangladesh by HVSR analysis: implications for engineering bedrock depth. *Journal of Applied Geophysics*, 211, 104967. https://doi.org/10.1016/J.JAPPGEO.2023.104967.

Farazi A.H., Ito Y., Soliman E., Garcia M., Lontsi A.M., José Sánchez-Sesma F., Jaramillo A. et al., 2023b. Shear wave velocity structure at the Fukushima forearc region based on H/V analysis of ambient noise recordings by ocean bottom seismometers. *Geophysical Journal International*, 233(3), 1801–1820. https://doi.org/10.1093/GJI/GGAD028.

FDSN, 2008. *BI: University of Dhaka Seismographic Network*. International Federation of Digital Seismograph Networks. https://www.fdsn.org/networks/detail/BI/ [access: 28.10.2021].

FDSN, 2011. *Z6 (2011–2017): PIRE: Life on a tectonically active delta in Bangladesh*. https://www.fdsn.org/networks/detail/Z6_2011/ [access: 28.10.2021].

Grecu B., Neagoe C., Tataru D., Borleanu F. & Zaharia B., 2018. Analysis of seismic noise in the Romanian-Bulgarian cross-border region. *Journal of Seismology*, 22(5), 1275–1292. https://doi.org/10.1007/s10950-018-9767-4.

Hasselmann K., 1963. A statistical analysis of the generation of microseisms. *Reviews of Geophysics*, 1(2), 177–210. https://doi.org/10.1029/RG001I002P00177.

Hossain M.S., Kamal A.S.M.M., Rahman M.Z., Farazi A.H., Mondal D.R., Mahmud T., Ferdous N., 2020. Assessment of soil liquefaction potential: a case study for Moulvibazar town, Sylhet, Bangladesh. *SN Applied Sciences*, 2, 777. https://doi.org/10.1007/s42452-020-2582-x.

Johnson S.Y. & Alam A.M.N., 1991. Sedimentation and tectonics of the Sylhet trough, Bangladesh. *GSA Bulletin*, 103(11), 1513–1527. https://doi.org/10.1130/0016-7606(1991)103<1513:SATOTS>2.3.CO;2.

Khan A.A. & Chouhan R.K.S., 1996. The crustal dynamics and the tectonic trends in the Bengal Basin. *Journal of Geodynamics*, 22(3–4), 267–286. https://doi.org/10.1016/0264-3707(96)00022-1

Lecocq T., Hicks S.P., Van Noten K., van Wijk K., Koelemeijer P., De Plaen R.S.M., Massin F. et al., 2020. Global quieting of high-frequency seismic noise due to COVID-19 pandemic lockdown measures. *Science*, 369(6509), 1338–1343. https://doi.org/10.1126/science.abd2438.

Longuet-Higgins M.S., 1950. A theory of the origin of microseisms. *Philosophical Transactions of the Royal Society of London. Series A, Mathematical and Physical Sciences*, 243(857), 1–35. https://doi.org/10.1098/rsta.1950.0012.

Mahmud M.I., Mia A.J., Islam M.A., Peas M.H., Farazi A.H. & Akhter S.H., 2020. Assessing bank dynamics of the Lower Meghna River in Bangladesh: an integrated GIS-DSAS approach. *Arabian Journal of Geosciences*, 13(14), 602. https://doi.org/10.1007/s12517-020-05514-4.

Marzorati S. & Bindi D., 2006. Ambient noise levels in north central Italy. *Geochemistry, Geophysics, Geosystems*, 7(9). https://doi.org/10.1029/2006GC001256.

McNamara D.E. & Buland R.P., 2004. Ambiente noise levels in the continental United States. *Bulletin of the Seismological Society of America*, 94(4), 1517–1527. https://doi.org/10.1785/012003001.

Molnar S., Cassidy J.F., Castellaro S., Cornou C., Crow H., Hunter J.A., Matsushima S. et al., 2018. Application of Microtremor Horizontal-to-Vertical Spectral Ratio (MHVSR) analysis for site characterization: State of the art. *Surveys in Geophysics*, 39(4), 613–631. https://doi.org/10.1007/s10712-018-9464-4.

Nakata N., Gualtieri L. & Fichtner A. (eds.), 2019. *Seismic Ambient Noise*. Cambridge University Press, Cambridge.

Ni J.F., Guzman-Speziale M., Bevis M., Holt W.E., Wallace T.C. & Seager W.R., 1989. Accretionary tectonics of Burma and the three-dimensional geometry of the Burma subduction zone. *Geology*, 17(1), 68. https://doi.org/10.1130/0091-7613(1989)017<0068:ATOBAT>2.3.CO;2.

Nishida K., 2017. Ambient seismic wave field. *Proceedings of the Japan Academy. Series B, Physical and Biological Sciences*, 93(7), 423–448. https://doi.org/10.2183/pjab.93.026.

Oakley D.O.S., Forsythe B., Gu X., Nyblade A.A. & Brantley S.L., 2021. Seismic ambient noise analyses reveal changing temperature and water signals to 10 s of meters depth in the critical zone. *Journal of Geophysical Research: Earth Surface*, 126(2), e2020JF005823. https://doi.org/10.1029/2020JF005823.

Peterson J., 1993. *Observations and Modeling of Seismic Background Noise*. Albuqueerque, New Mexico.

Pierson W.J. & Moskowitz L., 1964. A proposed spectral form for fully developed wind seas based on the similarity theory of S. A. Kitaigorodskii. *Journal of Geophysical Research*, 69(24), 5181–5190. https://doi.org/10.1029/JZ069I024P05181.

Rahman M.Z., Hossain M.S., Kamal A.S.M.M., Siddiqua S., Mustahid F. & Farazi A.H., 2018. Seismic site characterization for Moulvibazar town, Bangladesh. *Bulletin of Engineering Geology and the Environment*, 77(4), 1451–1471. https://doi.org/10.1007/s10064-017-1031-6.

Shapiro N.M., Campillo M., Stehly L. & Ritzwoller M.H., 2005. High-resolution surface-wave tomography from ambient seismic noise. *Science*, 307(5715), 1615–1618. https://doi.org/10.1126/science.1108339.

Singh A., Bhushan K., Singh C., Steckler M.S., Akhter S.H., Seeber L., Kim W.Y. et al., 2016. Crustal structure and tectonics of Bangladesh: New constraints from inversion of

receiver functions. *Tectonophysics*, 680, 99–112. https://doi.org/10.1016/j.tecto.2016.04.046.

Steckler M.S., Akhter S.H. & Seeber L., 2008. Collision of the Ganges-Brahmaputra Delta with the Burma Arc: Implications for earthquake hazard. *Earth and Planetary Science Letters*, 273(3–4), 367–378. https://doi.org/10.1016/j.epsl.2008.07.009.

Steckler M.S., Mondal D.R., Akhter S.H., Seeber L., Feng L., Gale J., Hill E.M. & Howe M., 2016. Locked and loading megathrust linked to active subduction beneath the Indo-Burman Ranges. *Nature Geoscience*, 9(8), 615–618. https://doi.org/10.1038/ngeo2760.

Uthaman M., Singh C., Singh A., Jana N., Dubey A.K., Sarkar S. & Tiwari A.K., 2022. Spatial and temporal variation of the ambient noise environment of the Sikkim Himalaya. *Scientific Reports*, 12(1), 274. https://doi.org/10.1038/s41598-021-04183-x.

Vassallo M., Festa G. & Bobbio A., 2012. Seismic ambient noise analysis in southern Italy. *Bulletin of the Seismological Society of America*, 102(2), 574–586. https://doi.org/10.1785/0120110018.

Webb S.C., 1998. Broadband seismology and noise under the ocean. *Reviews of Geophysics*, 36(1), 105–142. https://doi.org/10.1029/97RG02287.